

Quantitative Determination of the Catalytic Activity of Bulk Metal Oxides for Formic Acid Oxidation

David E. Fein and Israel E. Wachs¹

Zettelmoyer Center for Surface Studies, Department of Chemical Engineering, Lehigh University, Bethlehem, Pennsylvania 18015

Received June 5, 2001; revised May 15, 2002; accepted May 21, 2002

The dissociative chemisorption of formic acid, HCOOH, to surface formate species, HCOO-M, on metal oxide catalysts was examined. The chemisorption studies reveal an average of $\sim 5\text{--}6 \mu\text{mol}/\text{m}^2$ of active surface sites for many of the metal oxide catalysts. From TPD experiments, the decomposition temperatures of the surface formate (T_p) were found to vary from 88 to 313°C. The turnover frequency (TOF) values for formic acid oxidation were found to vary over 11 orders of magnitude ($10^{-3}\text{--}10^8 \text{ s}^{-1}$) at 250°C. No correlations were found between (i) H₂-TPR onset temperatures and the enthalpies of formation of bulk metal oxides ($-\Delta H_f$), (ii) TOFs and H₂-TPR onset temperatures, or (iii) TOFs and the isotopic dioxygen exchange rates with the metal oxide lattice oxygen. Weak inverse correlations were found for both TOFs and catalytic activities versus $-\Delta H_f$. A strong inverse relationship was found between the TOFs and the surface formate decomposition temperatures, supporting the assertion that the rate-determining step during formic acid oxidation is the decomposition of the surface formate intermediate.

© 2002 Elsevier Science (USA)

Key Words: formic acid; chemisorption; oxidation; metal oxide catalysts; TOF; TPD.

1. INTRODUCTION

The ability to quantitatively characterize surface catalyzed reactions is essential for understanding the activity of a wide range of catalytic materials. The importance of determining trends in reactivity for surface reaction intermediates on various catalysts is evident from the countless studies that have appeared on the development of a universal method for this purpose. From a review of the catalysis literature, it can be concluded that quantification of the number of active surface sites and turnover frequencies (TOFs: number of molecules converted per active surface site per second) and a measurement of surface reaction intermediate stability are required for the complete characterization of a catalytic material.

Several approaches have been previously proposed for quantifying the number of active sites on surfaces with various chemical probe molecules. Adsorption studies have

also been used extensively to determine the structure of the molecular or dissociatively adsorbed species with respect to coordination with the surface atoms (1–6). The most reliable method would, however, involve use of the actual reactant molecule with complementary chemisorption information obtained in the temperature region of the reaction (7). Additionally, the chemisorbed surface intermediate should be common on all of the catalytic materials and care should be taken to ensure that the surfaces of the catalysts are uniform in pretreatment as well as composition. Many researchers selected chemical probe molecules that were utilized to determine reaction rates and give insights into the quantity and nature of the active sites (1–14). For example, Ouyang *et al.* studied the chemisorption of pyridine, carbon dioxide, and formic acid to determine the acid–base properties of ZrO₂ (10). The decomposition of chemical probe molecules from the surface has also received wide spread attention due to its relationship to the adsorbed species (4, 8). While certain probe molecules can give insight into the acidic, basic, or redox nature of the surface active sites, the surface reactions should be identical on all samples for a truly unambiguous comparison of catalytic surfaces.

Formic acid (HCOOH) chemisorption satisfies all of the above criteria for appropriate selection of a probe molecule for catalytic comparisons. This molecule has been extensively employed in the past due to the commonality of the chemisorbed formate intermediate on nearly every catalytic surface. Furthermore, the surface formate intermediate is a very common intermediate in the water–gas shift reactions on the surface of metal oxides such as MgO, Al₂O₃, and ZnO (6).

As a vapor, formic acid will tend toward the *trans*-configuration due to its ability to dimerize; however, the dissociative adsorption is unimolecular and has a similar bonding structure on most oxide surfaces. Three surface bonding structures have been found for the surface formate intermediate: monodentate (Fig. 1a), bidentate (Fig. 1b), and surface bridged (Fig. 1c) configurations. It has been reported that under continuous flow conditions for NiO, the bidentate or bridged structures are formed to minimize surface energy (9). Similar findings were reported for the

¹ To whom correspondence should be addressed. Fax: (610) 758-5057.
E-mail: iew0@lehigh.edu.



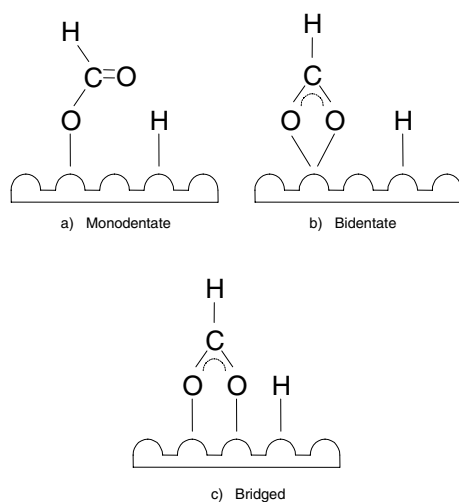


FIG. 1. Schematic of dissociative adsorption of formic acid on catalytic surfaces.

adsorption of formic acid onto the surface of ZrO_2 powder, where the bidentate surface formate species was identified (10), and for single-crystal $\text{MgO}(001)$ and $\text{TiO}_2(101)$, where the bridging and bidentate surface structures, respectively, were theoretically calculated to be more stable than the monodentate configuration (3, 5–6). However, analysis of the surface formate configuration from single-crystal metal oxide studies have revealed all possible configurations. Therefore, metal oxide powders would most likely exhibit an average of all configurations, depending on the most favorable disposition on a given crystal face. Although adsorption temperature can vary greatly for many compounds, it has been reported that formic acid is adsorbed on most metal and metal oxides surfaces dissociatively at room temperature to yield surface formate and surface hydroxyl species (6, 11). This same result has been confirmed by inelastic electron tunneling spectroscopic (IETS) studies for formic acid adsorption on the surface of Al_2O_3 (1).

The oxidation products of this simple carboxylic acid are identical on every surface since complete oxidation products, CO_2 and H_2O , are obtained. Despite single-crystal studies on $\text{MgO}(100)$ and $\text{SnO}_2(110)$, which have shown CO as a major product under ultrahigh-vacuum conditions (34), it has been found that the TOF values for CO oxidation on many metal oxides is typically $\sim 10^{-5} \text{ s}^{-1}$ at higher pressures (35). Any CO_2 observed is therefore a result of the adsorbed surface reaction, since the conversion of CO to CO_2 is too inefficient to significantly impact the results at higher pressures. In addition, the presence of diatomic oxygen in the gaseous reactant stream has been shown to exhibit very little effect on the temperature at which

products are formed for the decomposition or oxidation of formic acid (12). Therefore, TPO and TPD spectra for CO_2/HCOOH were shown to be almost identical in location, although much less CO and H_2 were formed during the temperature-programmed oxidation studies (12). Thus, it was concluded that the oxygen from the oxide surface itself reacts to form products, creating oxygen vacancies, which are then replaced by oxygen from the reactant stream via the Mars–van Krevelen mechanism. Based on these findings, it is possible to utilize the wealth of information describing surface formate decomposition temperatures from oxide surfaces to verify oxidation decomposition temperatures during formic acid oxidation experiments.

Traditionally, the focus has been to quantify the rate-determining step of surface reactions of chemical probe molecules. In the case of low conversion (<10%), the absence of diffusional effects makes it possible to study only the rate of the surface reaction without heat and mass transfer limitations (7). For surface formate intermediates, the rate-determining step for decomposition from the surface is the breaking of the C–H bond; therefore the decomposition temperature will be determined and employed as a measure of the intermediate stability and bonding strength to the surface. Additionally in the present study, bulk metal oxide samples were investigated due to their relatively high surface areas compared to that of pure metals. Powdered samples of the bulk metal oxides were employed in the present investigation, which represent an average of all crystal faces and most surely possess defects that are representative of samples used in practical applications as catalysts or supports.

In an attempt to illustrate Sabatier's principle of an ideally moderate intermediate stability, it has been reported that so-called "volcano curves" result from diagrams with a measure of the rate of a catalytic reaction along one axis and a measure of the stability of the putative intermediate compound on the other axis (13). In previous studies, the surface reaction rates, which are characteristic of the surface activity of a particular catalyst for a given reaction, were correlated with a bulk material property that was related to the stability of the intermediate compound (14). Thus, the objective of the present investigation is to consider only surface properties when making such correlations, since bulk material properties are not intrinsically related to the stability of the surface reaction intermediate.

2. EXPERIMENTAL

2.1. Catalyst Synthesis

The bulk metal oxide catalysts employed in the present investigation were either purchased as high-purity commercial chemicals or prepared by decomposition of their corresponding hydroxides or metal salts, as shown in Table 1. The

TABLE 1

Bulk Metal Oxide Catalyst Preparation

Catalyst	Source
MgO	MgCO ₃ , calcined at 350°C for 3 h, Aldrich
CaO	CaCO ₃ , calcined at 350°C for 3 h, Aldrich
SrO	Alfa Aesar, 99.5%
BaO	Ba(ClO ₄) ₂ · 3H ₂ O, calcined at 400°C for 3 h, Aldrich
Y ₂ O ₃	Alfa Aesar, 99.999%
La ₂ O ₃	Alfa Aesar, 99.999%
TiO ₂	Degussa P-25
ZrO ₂	Degussa
HfO ₂	Alfa Aesar, 99.9%
CeO ₂	Engelhard
V ₂ O ₅	NH ₄ VO ₃ , calcined at 450°C for 3 h, Alfa Aesar
Nb ₂ O ₅	Niobium Products Company
Ta ₂ O ₅	H. C. Starck Company
Cr ₂ O ₃	Alfa Aesar, 99.997%
MoO ₃	(NH ₄)Mo ₇ O ₂₄ · 4H ₂ O, calcined at 300°C for 5 h, Alfa Aesar
WO ₃	H ₂ WO ₄ , calcined at 400°C for 48 h, Aldrich
Mn ₂ O ₃	Mn(OOCCH ₃) ₂ , calcined at 250°C overnight, Alfa Aesar
Fe ₂ O ₃	Alfa Aesar, 99+%
Co ₃ O ₄	Aldrich
Rh ₂ O ₃	Rh(NO ₃) ₃ , calcined at 300°C for 4 h, Johnson Matthey
NiO	Ni(OH) ₂ , calcined at 230°C overnight, Alfa Aesar
PdO	Pd(NO ₃) ₂ , calcined at 300°C for 4 h, Johnson Matthey
PtO	Pt(NH ₃) ₄ Cl ₂ , calcined at 400°C for 4 h, Johnson Mathey
CuO	Cu(NO ₃) ₂ · 3H ₂ O, calcined at 200°C for 48 h, Johnson Matthey
Ag ₂ O	Alfa Aesar, 99%
Au ₂ O ₃	Au(OH) ₂ , calcined at 200°C for 48 h
ZnO	Aldrich, 99.97%
Al ₂ O ₃	Engelhard
Ga ₂ O ₃	Alfa Aesar, 99.999%
In ₂ O ₃	Alfa Aesar, 99.997%
SiO ₂	Carbosil EH-5
SnO ₂	Aldrich, 99%
Bi ₂ O ₃	Bi ₂ (C ₂ O ₄) ₃ , calcined at 400°C overnight, Alfa Aesar

pretreatment conditions of the precursors were obtained from the *Handbook of Chemistry and Physics* (15).

2.2. BET Surface Area

The BET surface area of each sample was determined by nitrogen adsorption/desorption isotherms on a Quantasorb surface area analyzer (Quantachrome Corporation, Model OS-9) using a 3:7 ratio of a N₂/He mixture. Typically, 0.2–0.3 g of sample was used for the measurement and the sample was outgassed at 250°C prior to N₂ adsorption at –195.8°C.

2.3. XPS Surface Analysis

The surface compositions of the group IB (Cu, Ag, and Au) oxide samples were examined to determine whether any surface impurities were present. A Scienta model ESCA-300 X-ray photoelectron spectrometer was employed for the surface composition measurements.

2.4. Formic Acid Chemisorption

The experimental conditions for quantifying the number of active surface sites via formic acid chemisorption were determined over a wide range of temperatures and formic acid partial pressures in a Cahn TGA microbalance (Model TG-131) coupled to a PC (Zenith Data Systems Model CW-282-82) for temperature and weight monitoring. A detailed flow diagram can be found in a prior publication (16). The system allowed for a controlled flow of high-purity gases: air for pretreatment, a mixture of formic acid and helium for chemisorption experiments, and pure helium for temperature-programmed decomposition experiments.

The following experimental procedure was employed, which accounts for all measurements associated with the TGA microbalance. After being weighed and loaded into the TGA, the oxide catalysts were heated *in situ* to 350°C for 1 h in flowing air (9.5 mL/min; ultrahigh purity; Air Gas) and helium (80 mL/min; ultrahigh purity; Air Gas) in order to remove adsorbed moisture and possible carbonaceous residues. The pretreated catalysts were then cooled in flowing helium to 100°C. Formic acid was quantitatively adsorbed onto the catalyst at 100°C from a flowing HCOOH/He stream (2000 ppm HCOOH; Scott Gas) for 1 h to obtain the weight gain. Previous surface formate adsorption studies on metal oxide surfaces (MoO₃) have shown that upon adsorption, H₂O formed from the combination of the chemisorbed hydrogen and oxygen atoms (36). The water formed is expelled from the surface due to water's weak interaction with the metal oxide surface. The net weight gain observed was subsequently corrected for loss of H₂O during HCOOH adsorption since one H₂O molecule is displaced from the surface during the dissociative adsorption of every two surface formate intermediates (16). The decomposition temperature of the surface formate intermediate was obtained by ramping the temperature at a constant rate of 10°C/min and monitoring the derivative of the weight loss.

The adsorption temperature for formic acid was 100°C since it was above the desorption temperature of physically adsorbed molecular formic acid, but below the decomposition temperature of the surface formate intermediates. The formic acid partial pressure also influenced the amount of physically adsorbed molecular formic acid that condensed on the catalyst pores, and 2000 ppm of formic acid in helium was found to essentially eliminate the condensation of molecular formic acid in the pores of the oxide catalysts at 100°C. Some of the pure metal oxide catalysts (CuO, PtO, PdO, Rh₂O₃, Au₂O₃, and Ag₂O) required lower adsorption temperatures, 50°C, because of catalysts reduction during HCOOH adsorption at 100°C.

2.5. Formic Acid Oxidation Reaction

Steady-state formic acid oxidation was used to examine the reactivity of the metal oxide catalysts. The reaction was

carried out in an isothermal fixed-bed differential reactor, which was held vertically and made out of Pyrex glass with a 6.2-mm outer diameter. Approximately 20 mg of catalyst was tested for formic acid oxidation at a number of temperatures for each sample at atmospheric pressure. The reactant gas mixture of HCOOH/He, molar ratio ~3.5/15.5/81, was used with a total flow rate of 100 mL/min. The gas feeds were controlled by mass flow controllers (Brooks Model 5850). Analysis of the reactor effluent was performed using an online gas chromatograph (HP 5890 series II) equipped with a thermal conductivity detector (TCD). A Porapak-QS packed column was used to separate the components prior to introduction to the TCD. The catalytic activities were calculated according to mole products per hour per square meter of catalyst.

2.6. Temperature Programmed Reduction (TPR) in H_2

TPR was carried out with an AMI-100 system (Zeton Altamira Instruments). A complete description of the apparatus can be found in a previous paper (7).

3. RESULTS

3.1. BET Surface Area Measurements and XPS Analysis

The surface areas of the pure metal oxide catalysts are presented in Table 2. The results reveal that the highest surface areas correspond to metal oxides that are typically used as supports (Al_2O_3 , TiO_2 , ZrO_2 , SiO_2 , CeO_2 , and Nb_2O_5). Purchased commercial catalysts were generally of low surface area with the exception of Fe_2O_3 ($21\text{ m}^2/\text{g}$), Ga_2O_3 ($18\text{ m}^2/\text{g}$), and Y_2O_3 ($27\text{ m}^2/\text{g}$), which showed comparatively higher surface areas. Since the BET experiments were run with N_2 adsorption, significant error might be associated with lower surface area ($<5\text{ m}^2/\text{g}$) samples.

Several metal oxides were analyzed by XPS to determine the composition of their surfaces. Of particular interest were Au_2O_3 , Ag_2O , and CuO since these catalysts exhibited extremely high activities. The XPS results revealed that the Au_2O_3 sample had a surface composition of primarily Au_2O_3 , with trace amounts of C, Cl, Au metal, and Na. The Ag_2O sample had a surface composition of primarily Ag_2O , with trace amounts of C and Na. The CuO sample had a surface composition of primarily CuO , with trace amounts of C and N. The absence of Pt and Pd impurities from all these surfaces reveals that the activity for formic acid oxidation is due entirely to the metal oxide surface.

3.2. Formic Acid Chemisorption

The oxidation of formic acid involves the dissociative chemisorption of formic acid to form reactive surface intermediates, as shown in Fig. 1. A precise determination of the maximum number of surface formate species formed during formic acid chemisorption is essential for quantifi-

TABLE 2
BET Surface Area and Bulk Heats of Formation ($-\Delta H_f$)

Catalyst	Surface area (m^2/g)	$-\Delta H_f^a$ (kcal/mol) (298 K) (33)
MgO	23	143.8
CaO	20	151.7
SrO	6	140.8
BaO	2	133.0
Y_2O_3	17	151.8
La_2O_3	5	179.7
TiO_2	50	107.1
ZrO_2	39	129.3
HfO_2	2	135.6
CeO_2	33	N.A.
V_2O_5	4	74.6
Nb_2O_5	55	N.A.
Ta_2O_5	4	97.2
Cr_2O_3	21	269.0
MoO_3	3	60.1
WO_3	15	65.2
Mn_2O_3	9	76.5
Fe_2O_3	21	66.2
Co_3O_4	3	49.0
Rh_2O_3	11	22.8
NiO	43	58.4
PdO	17	20.4
PtO	2	N.A.
CuO	1	38.5
Ag_2O	1	7.0
Au_2O_3	2	-11.0
ZnO	9	83.4
Al_2O_3	180	133.0
Ga_2O_3	18	86.6
In_2O_3	3	74.0
SiO_2	300	101.5
SnO_2	8	69.1
Bi_2O_3	4	45.7

^a Normalized per oxygen atom.

cation of the number of active surface sites available for formic acid oxidation. The adsorption temperature is an important consideration since only active surface sites are desired for activity calculations. It has been found that formic acid is dissociatively adsorbed on the ZnO surface at room temperature and any undecomposed formic acid was desorbed at 100°C (17). Associative formic acid adsorption was reported on NiO at 90 K, which then undergoes heterolytic dissociation upon heating to >200 K (4). Similar literature studies of HCOOH adsorption on the metal oxide surfaces have shown that adsorption temperatures below 100°C resulted in the coadsorption of surface formate intermediates and physically adsorbed molecular formic acid, and adsorption at temperatures significantly higher than 100°C resulted in the decomposition of surface formate intermediates (5, 18, 19). Therefore molecularly adsorbed species and decomposition of formate intermediates would alter the true number of surface active sites. Thus, 100°C was chosen as the adsorption temperature for formic acid since

it was above the desorption temperature of physically adsorbed molecular formic acid, at the temperature where formic acid readily dissociatively chemisorbed as surface formate intermediates, but below the decomposition temperature of the surface formate intermediates.

A series of pure metal oxides were examined for formic acid chemisorption and the results are presented in Table 3. The surface formate concentration is expressed as the number of accessible surface active sites per unit surface area (N_s). The number of surface formate species was calculated from the weight gain of the catalyst samples after adsorption of formic acid at 100°C. Several experiments were also conducted at 150°C to ensure that the weight gain corresponded to dissociative adsorption in the absence of molecular formic acid adsorption. Nearly identical values were obtained for TiO₂, Nb₂O₅, Fe₂O₃, and Al₂O₃, at both

100 and 150°C, which indicated that 100°C is an acceptable temperature for HCOOH dissociative chemisorption on most metal oxide surfaces.

Despite this generalization, chemisorption on certain metal oxides was conducted at 50°C. CuO required a lower adsorption temperature because it was reduced at the typical adsorption temperature of 100°C. Formic acid chemisorption on precious metal group oxides (PtO, PdO, Rh₂O₃, Ag₂O, and Au₂O₃) was also performed at 50°C due to the extremely reactive nature of these metal oxide surfaces at the typical adsorption temperature. A correction factor of 0.40 is obtained for metal oxides that require a lower adsorption temperature by comparing the surface active site density for TiO₂ at 50 and 100°C, since formic acid chemisorption at 50°C results in both molecular and dissociatively adsorbed formic acid. The extrapolated values of N_s for CuO, PtO, PdO, Rh₂O₃, Ag₂O, and Au₂O₃ at 100°C are also presented in Table 3.

The adsorption of formic acid on the metal oxide samples corresponds to \sim 5–6 $\mu\text{mol}/\text{m}^2$ HCOO_{ads} on average (excluding MgO, Ag₂O, ZnO, SrO, Bi₂O₃). The metal oxides MoO₃, V₂O₅, WO₃, and SrO all exhibited much lower values of N_s compared to the \sim 5–6 $\mu\text{mol}/\text{m}^2$ average seen on similar metal oxides. This suggests that either the number of exposed active surface sites for formic acid chemisorption is comparatively small or the formic acid molecules do not utilize the entire surface of these metal oxides. Prior studies have shown that alcohols only adsorb on the edges of the MoO₃ and V₂O₅ containing platelet morphologies (7). The extremely low value of N_s for SiO₂ is characteristic of the well-known unreactive nature of this oxide surface (7).

Significantly higher values of N_s were obtained for MgO, SrO, Ag₂O, ZnO, and Bi₂O₃. The results for these oxide surfaces reveal a much greater number of sites available for formic acid chemisorption. The number of active surface sites for SrO, Ag₂O, and Bi₂O₃ might be skewed due to the low BET surface areas for these samples that contain significant error. If the true surface area were higher, the number of active surface sites would decrease. The N_s values for MgO and ZnO are thought to be comparatively higher since these are basic catalysts, which could form bulk carbonates, thereby distorting the true active surface site value.

3.3. Decomposition Temperature of Surface Formate Species

In order to obtain a measure of surface stability of the surface formate species, the chemisorption experiments were extended to perform temperature-programmed decomposition (TPD). TPD studies resulted in the determination of the decomposition temperature of the surface formate species, since the adsorption studies were conducted in the absence of gas phase oxygen.

After dissociative adsorption of one monolayer of surface formate species was completed, the temperature was

TABLE 3

Surface Formate Decomposition Temperature (T_p) and Number of Active Surface Sites (N_s)

Catalyst	N_s ($\mu\text{mol}/\text{m}^2$)		HCOOH decomposition temp (°C)	
	50°C ^a	100°C ^a	150°C ^a	
MgO	—	83.0	—	306
CaO	—	7.3	—	313
SrO	—	20.9	—	248
BaO	—	7.5	—	309
Y ₂ O ₃	—	11.2	—	279
La ₂ O ₃	—	10.7	—	289
TiO ₂	9.7	3.9	4.0	228
ZrO ₂	—	2.0	—	246
HfO ₂	—	3.4	—	259
CeO ₂	—	4.1	—	280
V ₂ O ₅	—	1.6	—	216
Nb ₂ O ₅	—	3.4	3.4	242
Ta ₂ O ₅	—	8.2	—	255
Cr ₂ O ₃	—	6.8	—	217
MoO ₃	—	1.2	—	195
WO ₃	—	1.9	—	238
Mn ₂ O ₃	—	7.5	—	194
Fe ₂ O ₃	—	11.3	9.1	233
Co ₃ O ₄	—	4.1	—	190
Rh ₂ O ₃ ^b	8.8	4.4	—	178
NiO	—	6.5	—	220
PdO ^b	12.4	6.2	—	96
PtO ^b	8.3	4.1	—	88
CuO ^b	5.6	2.8	—	160
Ag ₂ O ^b	54.7	27.2	—	156
Au ₂ O ₃ ^b	5.1	2.5	—	136
ZnO	—	22.5	—	261
Al ₂ O ₃	—	6.3	5.2	230
Ga ₂ O ₃	—	5.5	—	181
In ₂ O ₃	—	5.6	—	254
SiO ₂	—	0.1	—	244
SnO ₂	—	7.0	—	229
Bi ₂ O ₃	—	123.2	—	257

^a Adsorption temperature.

^b Denotes adsorption data obtained at 50°C and corrected to 100°C.

ramped and the derivative of the weight loss versus temperature was analyzed for the maximum peak in the decomposition temperatures (T_p). The decomposition temperatures of the surface formate species for the various metal oxides catalysts examined are presented in Table 3. All of the metal oxides yielded only one decomposition peak, which occurred over a comparatively narrow range. The decomposition temperatures vary over a range of 225°C, with PtO exhibiting the lowest surface formate decomposition temperature (88°C) and CaO exhibiting the highest surface formate decomposition temperature (313°C). The oxides of precious metals (PtO, PdO, Ag₂O, Rh₂O₃, and Au₂O₃) as well as CuO exhibited relatively low surface formate decomposition temperatures (88–178°C). Among the transition metal oxides, Ga₂O₃, Co₃O₄, Mn₂O₃, and MoO₃ exhibited relatively low decomposition temperatures. The majority of the bulk metal oxides exhibited surface formate decomposition temperatures in the range 220–300°C.

3.4. Temperature-Programmed Reduction

Results were obtained from previous TPR studies for the same samples of metal oxides as were used in the present experiments (7).

3.5. Formic Acid Oxidation, Turnover Frequency, and Apparent Activation Energy

Surface formate groups are the surface intermediate species during the formation of fully oxidized reaction products (CO₂ and H₂O) during formic acid oxidation. Although formic acid can decompose in the vapor phase to a small extent at room temperature, partial oxidation products were not observed for any of the oxidation experiments. This was expected since the experiments were performed in excess oxygen. Also, since the adsorbed hydrogen atoms that are generated in the dissociative chemisorption process combine with adsorbed oxygen to form water, which subsequently desorbs due to weak interaction with the surface, it can be concluded that recombination of the hydrogen or hydroxyl groups with the surface formate does not occur. Therefore, all of the adsorbed formate species eventually react to produce CO₂ and H₂O.

Extensive testing was performed to ensure activity was only a function of temperature and not mass and heat transfer limitations. Significant apparent activation energies were found for the most active oxide catalysts (PtO, CuO, PdO), which mostly exhibited extremely low surface areas. Therefore, each sample was run at a series of temperatures while maintaining less than 10% conversion to ensure that mass and heat transfer limitations did not affect the rate expression. Thus, the HCOOH conversion as a function of catalyst temperature for each metal oxide sample was studied. This information was used to determine the activity of each metal oxide for formic acid oxidation at a common temperature. Of the 33 metal oxide catalysts studied, 25

showed activity in the temperature range between 200 and 300°C; therefore, the temperature of 250°C was chosen as the common temperature to compare the catalytic activities since most metal oxides showed reaction in this region. Only the six most active catalysts (Rh₂O₃, PdO, PtO, CuO, Ag₂O, Au₂O₃), BaO (305°C), and Bi₂O₃ (175°C) were active outside of the 100°C range targeted. The activities ranged from 1.9×10^{-2} to 1.7×10^9 ($\mu\text{mol}/\text{m}^2 \text{s}^{-1}$), with SiO₂ exhibiting the lowest activity and PdO the highest activity. The activities were spread out over the total range, with Bi₂O₃ exhibiting a relatively high activity 27 ($\mu\text{mol}/\text{m}^2 \text{s}^{-1}$) compared to that of the other samples (see Table 4).

TABLE 4

Formic Acid Oxidation Activities, Turnover Frequencies (TOF) at 250°C, Measured Ranges, Apparent Activation Energies (E_{app}), and Preexponential Factors

Catalyst	HCOOH activity (250°C) ($\mu\text{mol}/\text{m}^2 \text{s}^{-1}$)	TOF (s ⁻¹)	Measured temperature range (°C)	E_{app} (kcal/mol) ^a	Pre-exponential factors A (s ⁻¹) ^a
MgO	1.3	0.016	175–240	17	1.8E+07
CaO	0.081	0.011	210–310	10	8.7E+02
SrO	5.8	0.28	190–215	15	1.1E+07
BaO	0.047	0.0063	305–330	31	3.7E+11
Y ₂ O ₃	0.063	0.0057	260–290	20	1.2E+07
La ₂ O ₃	0.15	0.014	300–320	26	1.4E+10
TiO ₂	5.8	1.5	175–200	20	1.6E+09
ZrO ₂	0.27	0.14	175–205	10	2.5E+03
HfO ₂	0.58	0.17	225–275	25	2.6E+10
CeO ₂	0.12	0.028	200–260	6	5.0E+01
V ₂ O ₅	5.8	3.6	230–260	36	8.1E+15
Nb ₂ O ₅	2.6	0.78	175–200	18	9.4E+07
Ta ₂ O ₅	4.1	0.50	205–240	20	6.9E+08
Cr ₂ O ₃	0.84	0.12	200–235	13	1.7E+07
MoO ₃	5.4	4.3	170–225	11	3.1E+05
WO ₃	3.0	1.6	170–205	14	2.0E+06
Mn ₂ O ₃	20	2.7	180–200	36	1.5E+16
Fe ₂ O ₃	0.62	0.055	250–270	26	4.0E+10
Co ₃ O ₄	1.5	0.38	260–280	55	1.9E+23
Rh ₂ O ₃	3.0E+02	68	75–115	8	7.5E+05
NiO	29	4.4	200–215	44	6.3E+19
PdO ^b	1.7E+09	2.7E+08	35–50	28	1.0E+03
PtO ^b	4.9E+07	1.2E+07	30–50	16	2.1E+14
CuO	3.4E+03	1.2E+03	160–180	31	2.4E+16
Ag ₂ O	1.2E+02	4.4	90–160	4	3.7E+03
Au ₂ O ₃	1.0E+03	3.9E+02	45–80	13	1.7E+08
ZnO	0.047	0.0021	250–270	107	3.6E+43
Al ₂ O ₃	0.12	0.018	175–240	11	5.0E+03
Ga ₂ O ₃	0.64	0.12	200–265	9	4.4E+03
In ₂ O ₃	1.1	0.20	250–280	25	2.1E+10
SiO ₂	0.019	0.15	200–250	5	2.4E+00
SnO ₂	1.3	0.19	215–235	17	1.3E+07
Bi ₂ O ₃	27	0.22	145–175	11	1.1E+06

^a The values of E_{app} and A are only valid over the measured temperature ranges reported for each surface.

^b These metal oxide surfaces most likely encountered heat transfer limitations during the oxidation reaction due to unusually high catalytic activity. Extrapolated TOF values are estimated to be higher than the actual value by a factor of 10¹–10².

The commonality of the surface formate intermediate during dissociative chemisorption of formic acid and steady-state formic acid oxidation on metal oxide surfaces allows quantitative determination of the turnover frequency (TOF) values by normalizing the activities at 250°C to the number of active surface sites determined for each catalyst. For each metal oxide studied, all of the adsorbed surface formate intermediates reacted to form products in only one narrow temperature region. In the absence of multiple decomposition peaks, it can be concluded that active surface sites for the adsorption of the formate intermediate are identical to active surface sites for the oxidation reaction. The TOF values are shown in Table 4. The results reveal that formic acid oxidation TOF values vary over 11 orders of magnitude, from 10^{-3} to 10^8 s^{-1} . PdO exhibits the highest turnover frequency ($2.7 \times 10^8 \text{ s}^{-1}$) and ZnO the lowest ($2.1 \times 10^{-3} \text{ s}^{-1}$). Most of the precious metal oxides PtO ($1.2 \times 10^7 \text{ s}^{-1}$), PdO ($2.7 \times 10^8 \text{ s}^{-1}$), Rh₂O₃ ($6.8 \times 10^1 \text{ s}^{-1}$), and Au₂O₃ ($3.9 \times 10^2 \text{ s}^{-1}$), as well as CuO ($1.2 \times 10^3 \text{ s}^{-1}$), possess the highest turnover frequencies. Several transition metal oxide catalysts, TiO₂ ($1.5 \times 10^0 \text{ s}^{-1}$), V₂O₅ ($3.6 \times 10^0 \text{ s}^{-1}$), MoO₃ ($4.3 \times 10^0 \text{ s}^{-1}$), WO₃ ($1.6 \times 10^0 \text{ s}^{-1}$), Mn₂O₃ ($2.7 \times 10^0 \text{ s}^{-1}$), and NiO ($4.4 \times 10^0 \text{ s}^{-1}$), as well as Ag₂O ($4.4 \times 10^0 \text{ s}^{-1}$), also exhibited comparatively high turnover frequencies. In addition to ZnO, comparatively low turnover frequencies were demonstrated by BaO ($6.3 \times 10^{-3} \text{ s}^{-1}$) and Y₂O₃ ($5.7 \times 10^{-3} \text{ s}^{-1}$).

In addition to the activity data at the common temperature of 250°C, the conversion at each temperature was used to construct an Arrhenius plot of HCOOH oxidation for each catalyst. The E_{app} values ranged from 4 to 107 kcal/mol, with Ag₂O exhibiting the lowest value and ZnO exhibiting the highest (Table 4). The majority of the metal oxides studied exhibited apparent activation energies in the range 10–36 kcal/mol. Comparatively low apparent activation energies were shown by CeO₂ (6 kcal/mol), Rh₂O₃ (8 kcal/mol), Ag₂O₃ (4 kcal/mol), SiO₂ (5 kcal/mol), and Ga₂O₃ (9 kcal/mol). The highest values were shown by Co₃O₄ (55 kcal/mol), NiO (44 kcal/mol), and ZnO (107 kcal/mol). The preexponential factor for each surface was also calculated and values for A ranged from 2.4×10^0 to 3.6×10^{43} , with SiO₂ exhibiting the lowest value and ZnO the highest (Table 4). The majority of the metal oxides exhibited preexponential factors between 1.0×10^3 and 2.4×10^{16} . Comparatively low values are noted for SiO₂ (2.4×10^0), CeO₂ (5.0×10^1), and CaO (8.7×10^2), and high values for NiO (6.3×10^{19}), Co₃O₄ (1.9×10^{23}), and ZnO (3.6×10^{43}).

3.6. Correlations

The quantitative techniques employed in the analysis of these samples resulted in values for N_s (number of active surface sites), T_p (decomposition temperature), E_{app} values,

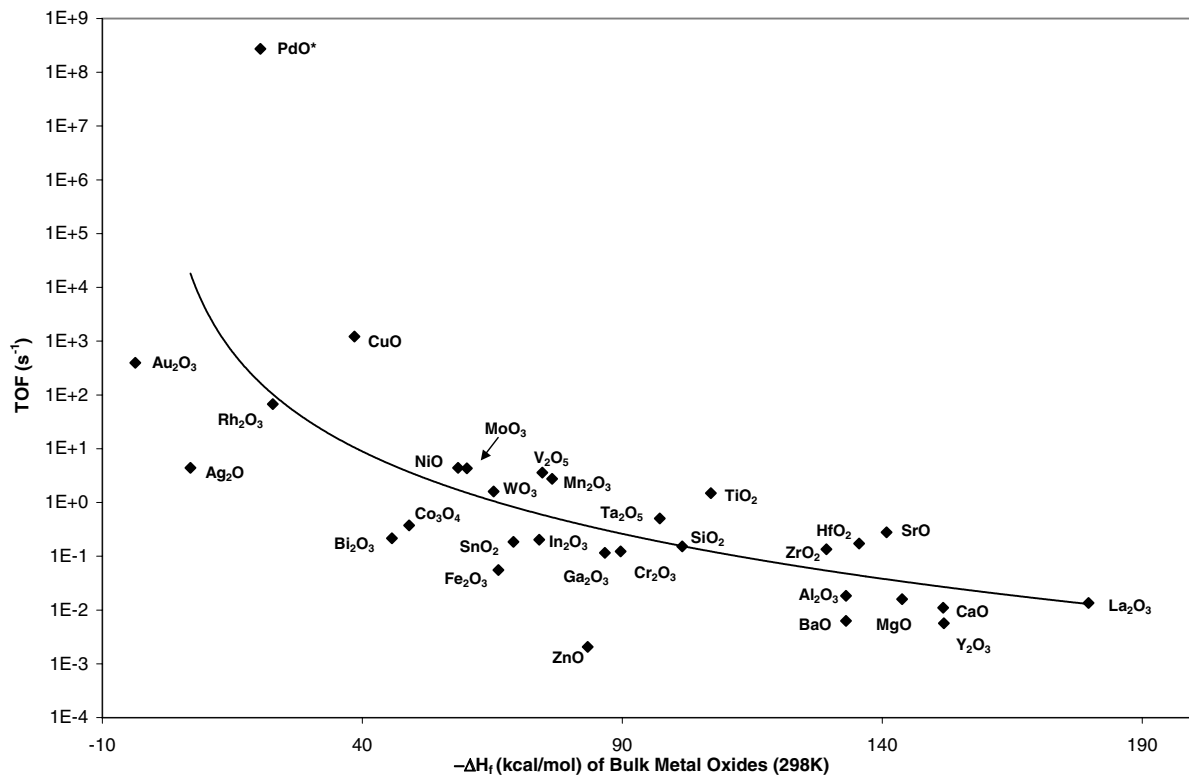
A (preexponential factor), and activity for formic acid oxidation for each oxide catalyst. The extensive set of formic acid activity and number of active surface site data allowed the determination of the intrinsic TOFs of the different catalysts, which can be correlated with other catalytic parameters to obtain additional fundamental insights about these bulk metal oxide catalysts for formic acid oxidation.

3.6.1. Turnover Frequency Correlations

Formic acid oxidation TOFs are plotted against the enthalpies of formation of selected bulk metal oxides ($M_x O_y$) normalized per mole of oxygen atom (see Fig. 2). The TOFs do not appear to correlate with the bulk metal–oxygen bond strength, however, a very weak correlation is seen that suggests that TOF decreases with increasing ΔH_f for the bulk metal oxides. The temperature required to reach a constant activity of $31.6 (\mu\text{mol}/\text{m}^2 \text{ s}^{-1})$ for HCOOH oxidation for each oxide catalyst is plotted against the enthalpies of formation in Fig. 3. Note that the temperatures are plotted inversely to emphasize that more active catalysts require lower reaction temperatures to achieve this activity. This plot again resulted in a weak correlation, suggesting that activity decreases with increasing ΔH_f for the bulk metal oxides. The onset temperatures for H₂ reduction were plotted against the enthalpies of formation for the available metal oxide samples in Fig. 4, and no correlation was obtained. The TOF values were also plotted against the onset temperature for reduction, obtained from H₂-TPR of the bulk metal oxide catalysts, which is shown in Fig. 5. However, no correlation was found between TOF and H₂-TPR onset temperature for reduction. The isotopic dioxygen exchange rate constants for the available metal oxides were obtained from Boreskov (20), at a common temperature of 300°C, and normalized to the surface area of each sample. The TOFs were plotted against the isotopic dioxygen exchange rate constant K (molecules/cm² s⁻¹), in Fig. 6, for selected metal oxide catalysts with no apparent correlation. A strong inverse relationship was found to exist between the formic acid oxidation TOFs and the surface formate intermediate decomposition temperatures, as shown in Fig. 7. A plot of the preexponential factor against E_{app} shows a strong relationship, as shown in Fig. 8.

4. DISCUSSION

The results presented above reveal both qualitative and quantitative information about the intrinsic activity of bulk metal oxide catalysts for formic acid chemisorption and oxidation and their relationship to other thermodynamic and kinetic parameters. It has previously been shown by *in situ* Raman spectroscopy that during the oxidation of methanol, the surfaces of Rh, Pd, and Pt metals remain oxidized as Rh₂O₃, PdO, and PtO respectively (21–23). A similar finding was reported for *in situ* Raman spectroscopy studies



* Extrapolated TOF value estimated higher than the actual value by a factor of 10^1 - 10^2 due to heat transfer limitations

FIG. 2. Semilog plot of TOF vs enthalpy of formation of bulk metal oxide catalysts.

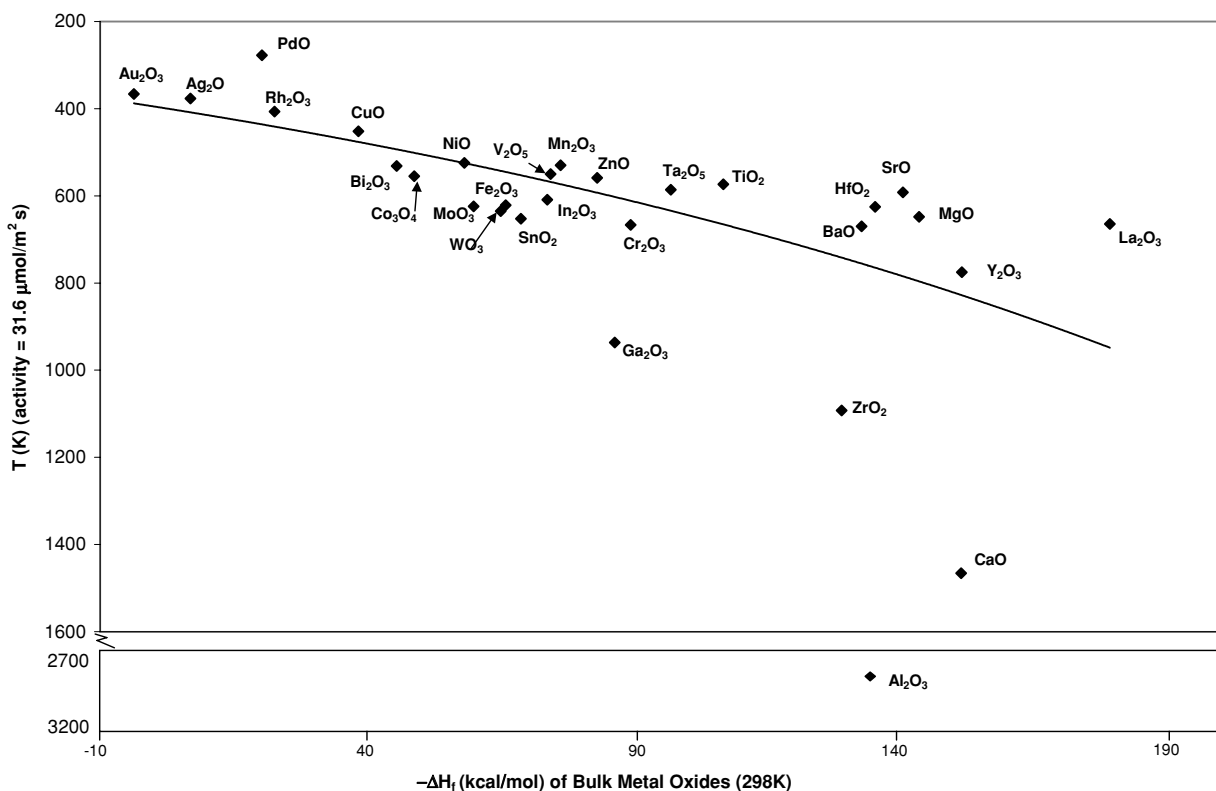


FIG. 3. Plot of temperature to achieve activity of $31.6 \mu\text{mol}/\text{m}^2 \text{s}^{-1}$ (reverse order) vs enthalpy of formation of bulk metal oxide catalysts.

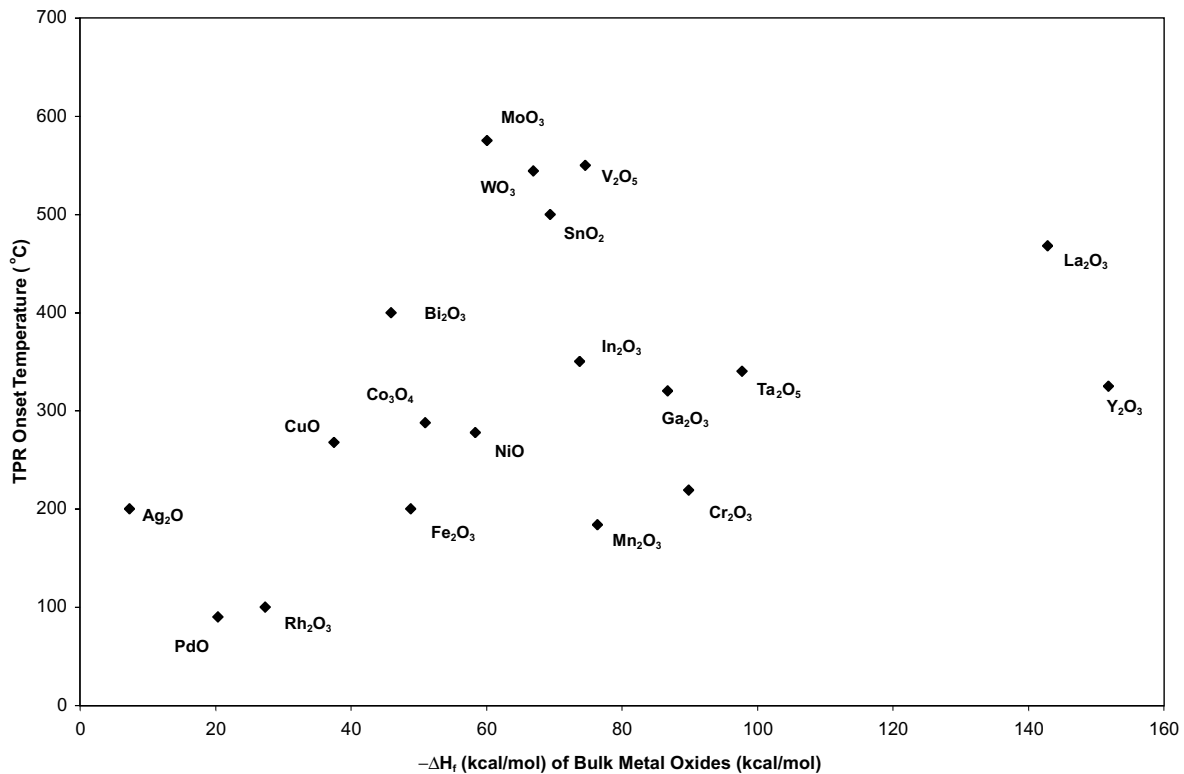
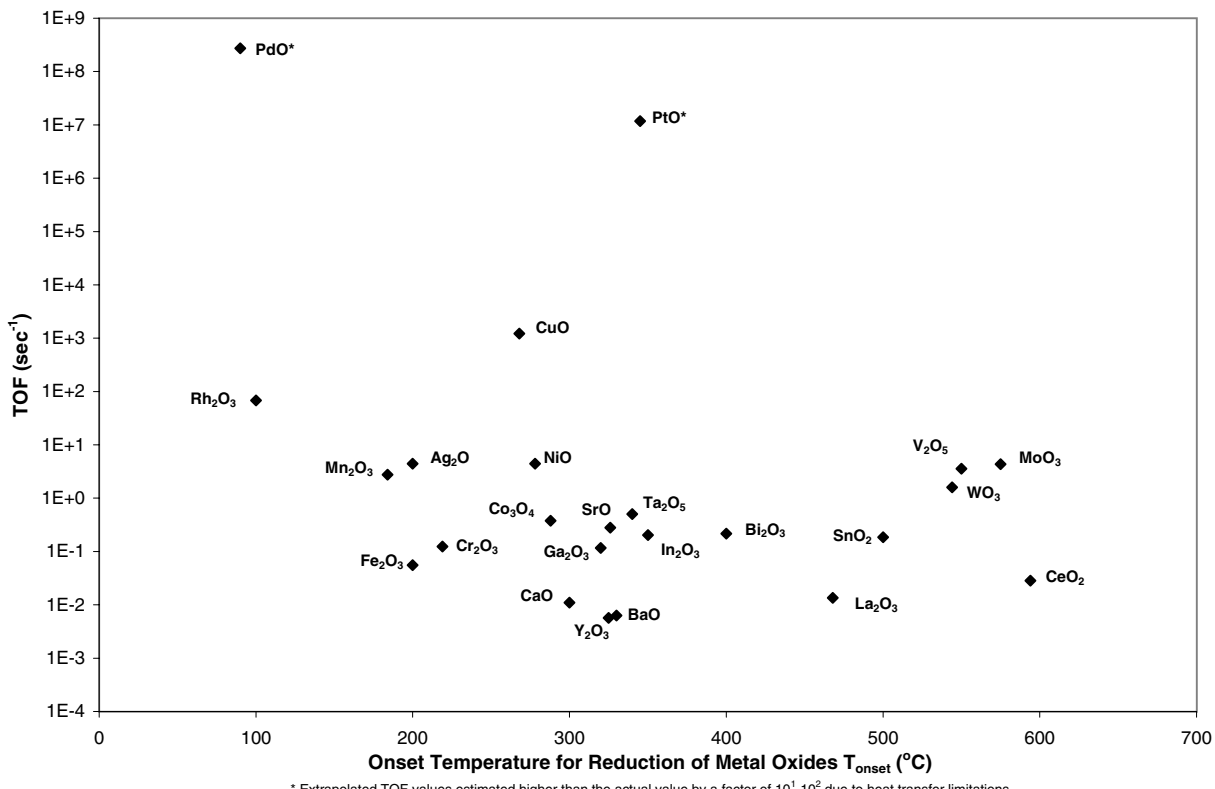


FIG. 4. Plot of onset temperature for reduction of metal oxides vs enthalpy of formation of bulk metal oxide catalysts.



* Extrapolated TOF values estimated higher than the actual value by a factor of 10^1 - 10^2 due to heat transfer limitations

FIG. 5. Semilog plot of TOF vs onset temperature for reduction of metal oxides.

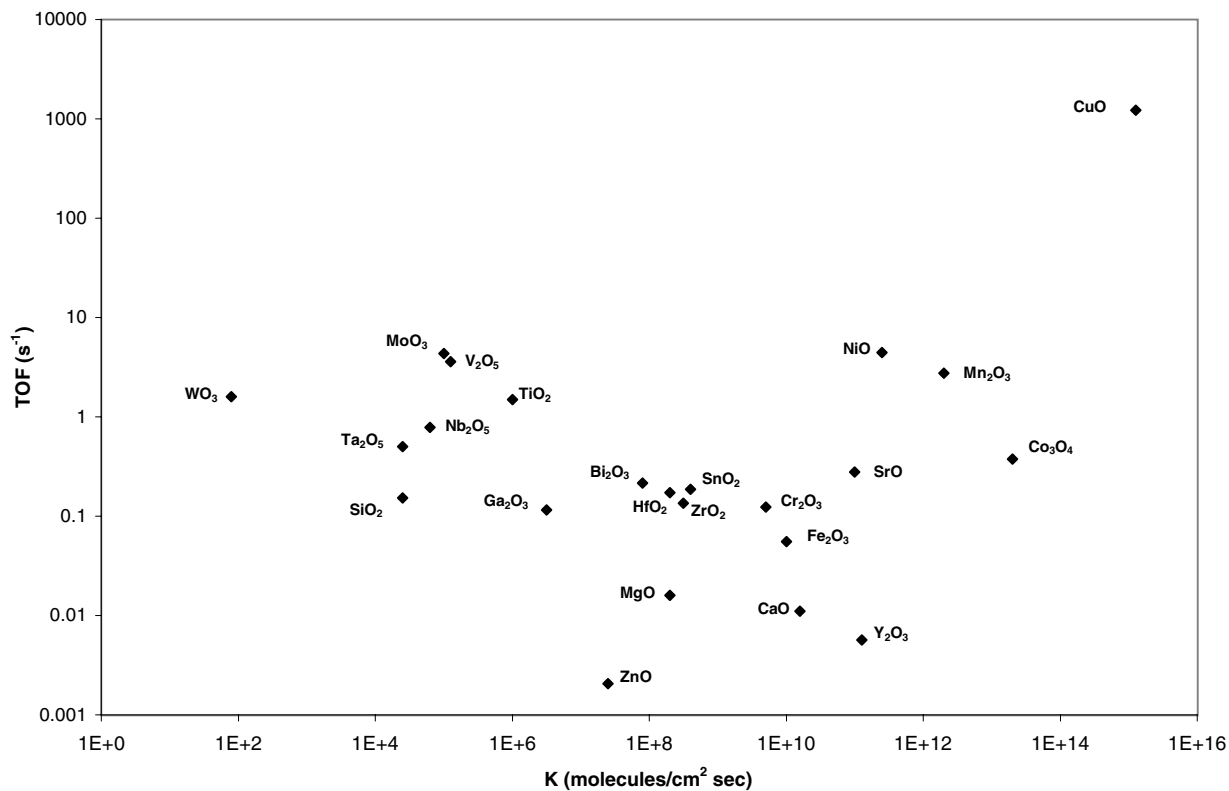
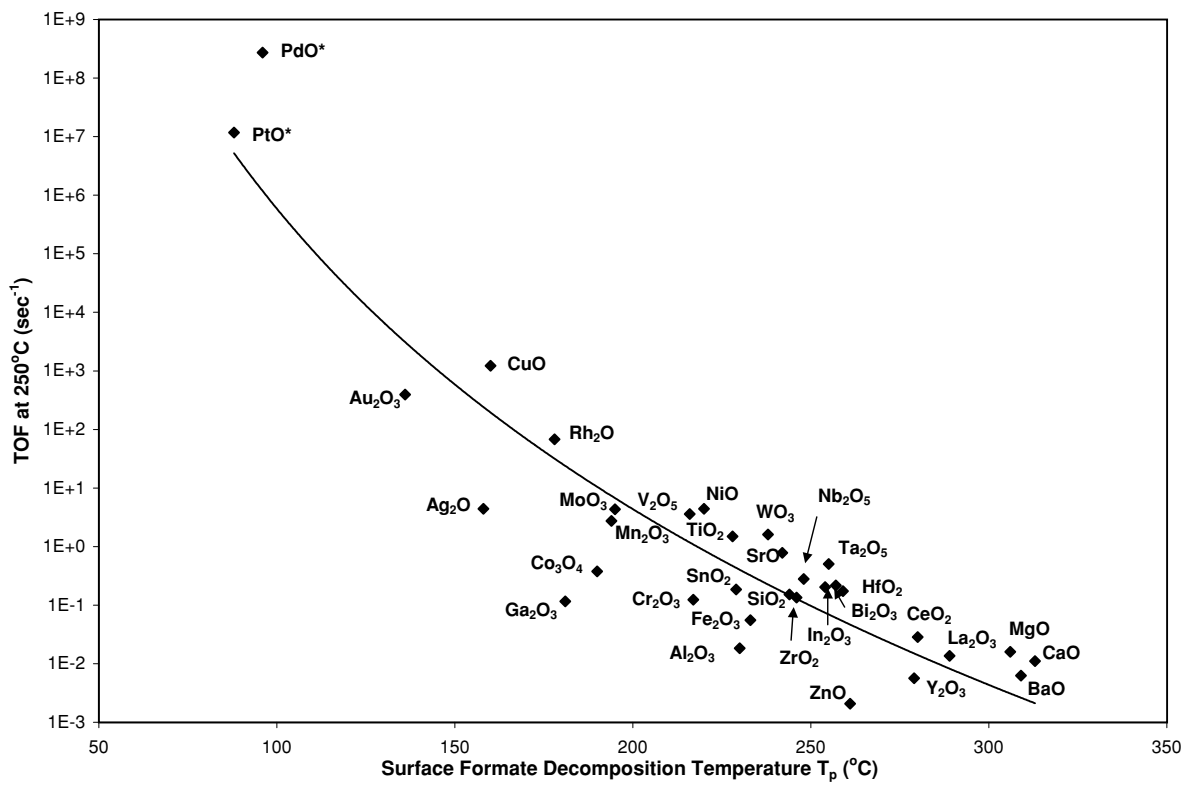


FIG. 6. Log-log plot of TOF vs isotopic dioxygen exchange rate constant.



* Extrapolated TOF values estimated higher than the actual value by a factor of 10^1 - 10^2 due to heat transfer limitations

FIG. 7. Semilog plot of TOF vs surface formate decomposition temperature.

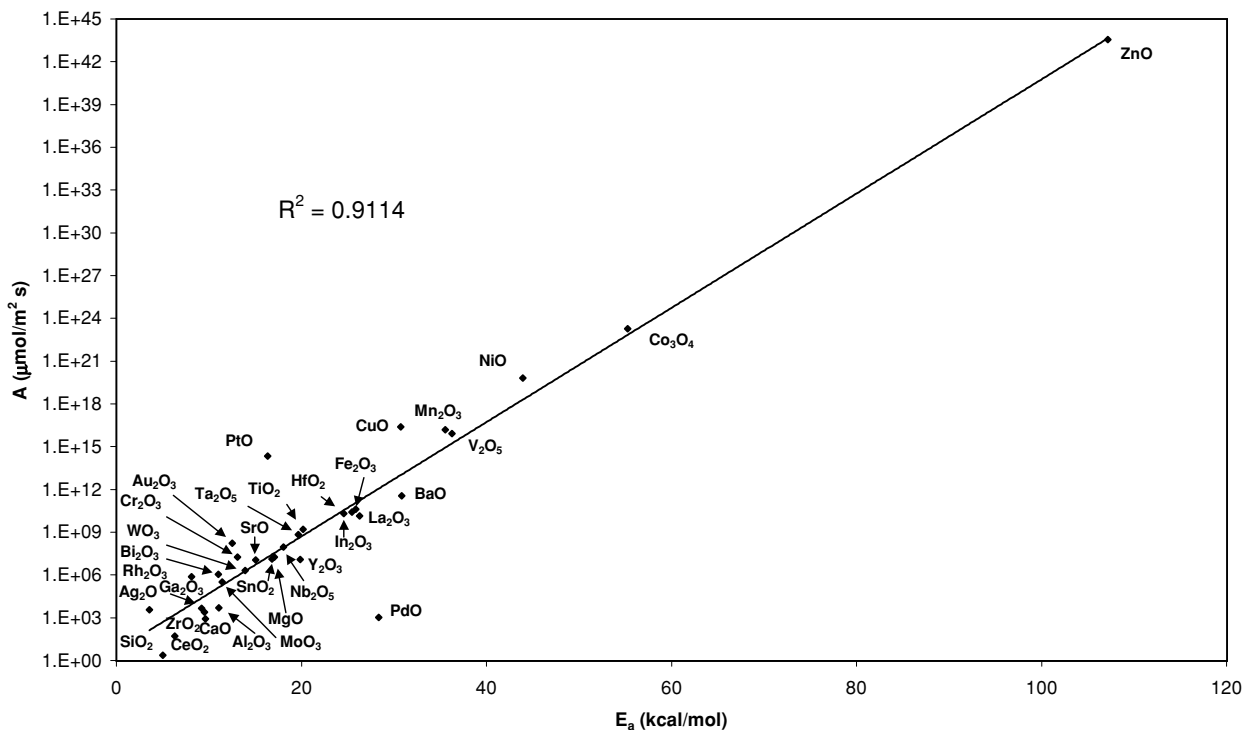


FIG. 8. Semilog plot of preexponential factor vs apparent activation energy.

performed during the oxidation of methanol over polycrystalline Ag (24) and for X-ray absorption spectroscopy of methanol oxidation over Cu (25, 26). Analogous *in situ* Raman observations were also made with V₂O₅ and MoO₃ during methanol oxidation (27). It can be concluded that the surfaces of all of the metal oxide catalysts examined in the present study are also oxidized since methanol and formic acid both lose two hydrogen atoms during their oxidation to H₂CO and CO₂, respectively. This conclusion is further supported by the fact that the present investigation employs excess oxygen (O₂-to-formic-acid ratio of 13:3). Thus, the excess gas-phase oxygen serves to ensure complete surface oxidation under the current reaction conditions.

Formic acid chemisorption provides the number of surface active sites for bulk metal oxide catalysts. Since most catalytic solids are polycrystalline, each particle may possess vacancies and defects with a different number of active surface sites. The chemisorption method employed in this experiment enables the determination of an average active surface site density for the bulk metal oxides. It has been shown that all adsorption sites are occupied by formic acid chemisorption on TiO₂ at monolayer coverages (28). Thus, the number of active surface site values represents the maximum number of sites that can chemisorb a surface formate species and hydroxyl species for a given surface, taking into account steric interactions as well as available surface area.

The quantitative values for the number of active surface sites for formic acid chemisorption onto metal oxide

surfaces agree with the limited amount of previous data reported for similar studies (see Table 5). Based on these findings, it can be concluded that the values agree very well within experimental error for metal oxides presented for the different methods employed to determine the number of active surface sites.

The most important benefit of calculating active surface site densities is that different bulk metal oxide catalysts with broadly varying surface areas can be normalized and compared explicitly through their turnover frequencies. Comparison of the number of active surface sites for bulk metal oxides yields similar adsorption surface site densities for the majority of samples studied, ~5–6 μmol HCOO_{ads}/m². This indicates the similar tendencies for the metal oxide catalytic surfaces to dissociatively chemisorb formic acid despite the various surface arrangements. In addition, catalyst preparation conditions do not appear to play a critical role in the

TABLE 5
Active Surface Site Comparison to Reported Literature Values

Catalyst	Reported number of active sites	Present study calculation
TiO ₂ (powder)	2.3 μmol/nm ² (2)	3.9 μmol/nm ²
ZrO ₂ (powder)	1.0 μmol/m ² (10)	2.0 μmol/m ²
ZnO	8.7 μmol/m ² , crystal faces: (100), (010), (001) (11)	22.5 μmol/nm ² (powder)

active surface site density since most samples were prepared under various conditions and exhibit similar values.

In comparison to analogous studies performed using other chemical probe molecules for metal oxide chemisorption, there also appears to be similar values for the active surface site density. For methanol (CH_3OH) chemisorption, most metal oxide catalysts were shown to exhibit $\sim 3\text{--}4 \mu\text{mol } \text{CH}_3\text{O}_{\text{ads}}/\text{m}^2$ on average (7). Thus, it appears that the majority of metal oxides demonstrate comparable numbers of active surface sites for the dissociative adsorption of small chemical probe molecules.

The surface formate decomposition temperature, as obtained from the TPD studies for each metal oxide sample, was used as the measure of surface formate stability, which is strictly a surface property. According to Poulston *et al.*, a main surface formate decomposition peak to CO_2 from CuO is observed at 272°C , with a minor peak at 157°C (29). The present analysis revealed a primary decomposition peak at 241°C and a minor peak at 160°C . The latter formate decomposition temperature, which would be achieved first during steady-state kinetic studies in which the temperature is ramped until oxidation products are observed, is nearly identical to the value reported by Poulston *et al.* TPD experiments for formate decomposition on ZnO were also compared with literature values and found to be similar. It has been reported that the decomposition of the surface formate intermediate occurs at about 200°C for the surface of $\text{ZnO}(0001)$ under ultrahigh-vacuum (UVH) conditions (17), compared to 261°C observed for powdered ZnO in the present study. Low formic acid exposures resulted in decomposition of the surface formate intermediate to CO_2 and H_2O at 202°C for $\text{TiO}_2(110)$ (8). The decomposition temperature obtained in the present study for a powder TiO_2 sample was 237°C , which is similar to that obtained in the single-crystal study. The present analysis exhibits accurate decomposition temperatures for powder metal oxide catalysts, which represent the average of all crystal faces and are used to quantify the surface formate intermediate stability.

Formic acid oxidation over the bulk metal oxide catalysts yielded exclusively CO_2 and H_2O . Therefore, selectivity of a particular surface toward the production of partial oxidation products (either H_2 and CO_2 or H_2O and CO), as seen in formic acid decomposition studies, did not play a factor in the present investigation. Oxidation was more suitable for comparison purposes since certain metal oxide surfaces exhibit all of these products for formic acid decomposition (8, 9, 17, 19). Thus, all the active surface sites determined from the chemisorption studies can be assumed to contribute to the activity of the metal oxide catalyst for formic acid oxidation to CO_2 and H_2O . The average activity of a surface site for a particular metal oxide is reported as a TOF.

Comparison of the formic acid TOF values at 250°C over the metal oxide catalysts reveals that they vary over 11

orders of magnitude, from 10^{-3} to 10^8 s^{-1} . These values represent a true catalytic parameter for a given metal oxide catalytic surface toward formic acid oxidation. Thus, the TOF values can be compared to other catalytic parameters explicitly since they embody an accurate normalized surface property of the metal oxide surfaces.

Kinetic studies of formic acid oxidation also made possible the determination of the apparent activation energies and preexponential factors for the various metal oxide catalysts for formic acid oxidation. These apparent activation energies are not corrected for the enthalpy of adsorption (30); however, they do give insight into the strength of chemisorption of the surface intermediate formate species. Although previous studies have reported apparent activation energies for formic acid decomposition on metal oxide catalysts, no information could be found in the literature for steady-state oxidation experiments. Therefore, the calculated values are presented (Table 4) without comparison to previous literature values.

To determine the effect of heat transfer on the oxidation of formic acid for the metal oxide surfaces, a plot of the preexponential factor versus the apparent activation energy was constructed (Fig. 8). This plot clearly shows a direct correlation between these parameters, as would be expected as a compensation effect for the activity of each of the surfaces. The two catalysts exhibiting the highest activity, PdO and PtO , deviate most significantly from the linear correlation. It can be assumed that these surfaces most likely encountered heat transfer limitations during the oxidation reaction due to their unusually high catalytic activity. Based on a comparison of the experimental results for PdO and PtO to the majority of the metal oxides studied, the calculated TOF values for these two surfaces are estimated to be higher than the actual value by a factor of $10^1\text{--}10^2$. Note that due to the unusually high activity demonstrated for formic acid oxidation by these surfaces, any overstatement in the reported values not corrected for heat transfer limitations will not affect any of the correlations, trends, or conclusions discussed in this study. Also, the reported values for both E_a and A are only accurate over the measured temperature range for each surface for formic acid oxidation. Any extrapolation outside of these narrow ranges will introduce error and will not be representative of the actual values at the desired temperature. However, for the purpose of this study it is important to recognize that the measured temperature range for each surface is very close to the desired normalization point of 250°C ; therefore the reported values for both E_a and A apply directly.

Correlation of the TOF values with other catalytic parameters may provide fundamental insights into these bulk metal oxide catalysts for the formic acid oxidation reaction. Figure 2 demonstrates that a very weak inverse correlation results from the plot of TOF versus the bulk heat of formation of the metal–oxygen bond strength of the metal oxide.

Thus, TOF qualitatively decreases with increasing $-\Delta H_f$ for the bulk metal oxides. No correlation is seen for metal oxides with moderate-to-high bulk enthalpies of formation. It was previously stated that there appears to be a correlation between the bulk heats of formation of the metal oxide catalysts divided by the number of oxygen atoms and the catalytic activity toward the total oxidation of some chemical compounds (31). However, the surface reaction rates, which are characteristic of the *surface* activity of a particular catalyst for a given reaction, should not be inherently related to a *bulk* material property of the metal oxide catalytic material. Thus, when the rate of a catalytic reaction is plotted versus the stability of the metal–oxygen bond strength, no correlation is expected, although a weak qualitative relationship is seen.

Figure 3 shows a weak inverse correlation between the inverse temperature to achieve a constant catalytic activity and the bulk metal–oxygen bond strength, suggesting that activity decreases with increasing $-\Delta H_f$ for the bulk metal oxides. The existence of the correlation is explained with the same reasoning that can be applied for the TOF versus $-\Delta H_f$ correlation seen in Fig. 2. One possible explanation for the low activity of Al_2O_3 is that it is known to form surface carbonates as high as 300°C, which would inhibit chemisorption HCOOH (32). It was previously shown that a plot of the temperature required for a surface to achieve a particular rate of activity in reverse order versus a bulk property will exhibit “volcano curve” behavior for a range of materials (14). However, when the surface catalytic activity is plotted against the bulk metal–oxygen bond strength, one would not expect a correlation since this would represent a correlation of surface and bulk material properties. An important feature of Fig. 3 is that although the temperature required to reach a constant activity increases with the bulk metal–oxygen bond strength, no “volcano curve” is obtained.

Temperature-programmed reduction ($\text{H}_2\text{-TPR}$) studies are commonly used to reflect the ease of oxygen removal from metal oxide catalysts. The onset temperature for reduction corresponds to either the dissociative adsorption of molecular H_2 or the recombination of surface hydroxyls to form H_2O , which may vary among the different metal oxide catalysts. When the onset temperature for reduction of the metal oxide catalysts is plotted against the bulk metal–oxygen bond strength, as shown in Fig. 4, no correlation exists.

The TOF values are plotted against the $\text{H}_2\text{-TPR-}T_{\text{onset}}$ of the metal oxide catalysts in Fig. 5. Each of these parameters uses a different chemical probe molecule to quantify the $\text{H}_2\text{-TPR-}T_{\text{onset}}$. The onset temperature for reduction uses H_2 to establish the rate-determining steps of either H_2 dissociative adsorption or hydroxyl recombination on the surface, while TOF values were calculated using formic acid as the probe molecule and depend on the breaking of the C–H bond as the rate-determining step during HCOOH oxida-

tion. Therefore, no correlation should exist between a plot of these two parameters, as shown.

Figure 6 shows no correlation when the TOFs were plotted against the isotopic dioxygen exchange rate constant K ($\text{molecules/cm}^2 \text{ s}^{-1}$). The isotopic dioxygen exchange rate constant K ($\text{molecules/cm}^2 \text{ s}^{-1}$) is characteristic of the rate of exchange of bulk lattice oxygen molecules per unit surface per unit time for a metal oxide. The dioxygen exchange rate constant represents the exchange between gas phase oxygen and the surface and bulk lattice oxygen atoms of the metal oxide catalysts (20). This exchange rate, although it does play a role in the Mars–van Krevelen mechanism for oxidation from these surfaces, is not the rate-determining step for formic acid oxidation. TOF values are dependent on the decomposition of the surface formate intermediate, which is characteristic of the breaking of the C–H bond representing the rate-determining step for the reaction. Therefore, since these measures of surface properties do not correspond to the same step in the reaction mechanism, one should not expect that a correlation exists between TOF and the isotopic dioxygen exchange rate.

The TOF values were also plotted against the surface formate decomposition temperatures obtained from the TPD studies (see Fig. 7). Both the oxidation TOF and the TPD decomposition temperature proceed by means of the same rate-determining step, the decomposition of the surface formate intermediate. Although the plot is semilog in order to show the 11 orders of magnitude change in the TOF values, a qualitative inverse relationship is obtained between the TOF values and the decomposition temperatures of the surface formate intermediates. This result indicates that the thermal stability of the surface formate intermediate is the only significant kinetic parameter. Thus, dissociative adsorption of formic acid is not kinetically significant during HCOOH oxidation over metal oxide catalysts. Similar findings were reported when methanol was used as the chemical probe molecule for the same set of metal oxide catalysts (7).

The data in Fig. 7 demonstrate that only the right-hand side of the classic “volcano plot” (14) is obtained when the TOF is plotted against the surface formate decomposition temperature. It has been proposed that these classic “volcano plots” suggest that there is a shift in the rate-determining step of the reaction as one crosses from the “left-hand” side to the “right-hand” side of the plot. The catalysts on the left side of the curve exhibit adsorption limiting behavior. Consequently, the corresponding reaction rate is small since the reactant molecules are not readily dissociatively adsorbed onto the active surface sites. On the right side of the curve, decomposition from the surface has been proposed to be the rate-limiting process. These surfaces dissociatively adsorb the reactant easily; however, the bond to the surface is very strong, thereby limiting the reaction rate since surface reaction and desorption are

necessary for products to be formed. Compounds at the peak of the volcano curve, commonly precious metal catalysts, exhibit an optimal balance of intermediate stability as put forth by Sabatier and, therefore, should exhibit the highest rates of reaction (13). These classical interpretations are likely correct for surface reactions where the adsorption of chemical probe molecules on the catalyst surface is an activated process, but these interpretations do not appear to hold for surface reactions where adsorption is relatively easy and the decomposition of the surface intermediate is the rate-determining step (see Fig. 7). Similar findings were also reported for analogous methanol oxidation studies over bulk metal oxide catalysts (7).

5. CONCLUSIONS

The catalytic oxidation of formic acid on bulk metal oxides was studied using (i) dissociative chemisorption to form surface formate intermediates for determination of the number of active surface sites, (ii) temperature-programmed desorption to obtain the surface formate intermediate decomposition temperatures, and (iii) steady-state oxidation kinetic studies to calculate TOFs. Comparison of the number of active surface sites for bulk metal oxides yields similar adsorption surface site densities for the majority of samples studied, $\sim 5\text{--}6 \mu\text{mol HCOO}_{\text{ads}}/\text{m}^2$. Kinetic studies of formic acid oxidation made possible the determination of the apparent activation energies for the various metal oxide catalysts for formic acid oxidation. The TOF values for the various metal oxide catalysts studied were found to vary over 11 orders of magnitude ($10^{-3}\text{--}10^8 \text{s}^{-1}$). The variation in TOF values was not related to the isotopic dioxygen exchange rate constant or the onset temperature for reduction of the metal oxide surfaces. Weak inverse correlations were seen between TOF and activity and the bulk metal–oxygen bond strength, however, a “volcano curve” over the range of bulk metal oxide catalysts was not observed. A strong inverse relationship was found between the TOF values and the decomposition temperatures of the surface formate intermediates. This result indicates that the thermal stability of the surface formate intermediate is the only significant kinetic factor. Thus, dissociative adsorption of the formic acid molecule is not kinetically significant for kinetic activity during formic acid oxidation over the metal oxide catalysts. Consequently, it is concluded that one must consider only surface properties when attempting to establish correlations for catalytic parameters.

ACKNOWLEDGMENT

The support of the Lehigh University Presidential Scholar's Program is gratefully acknowledged.

REFERENCES

- Lewis, B. F., Mosesman, M., and Weinberg, W. H., *Surf. Sci.* **41**, 142 (1974).
- Root, T. W., and Duncan, T. M., *J. Catal.* **101**, 527 (1986).
- Vittadini, A., Selloni, A., Rotzinger, F. P., and Gratzel, M., *J. Phys. Chem. B* **104**, 1300 (2000).
- Truong, C. M., Wu, M. C., and Goodman, D. W., *J. Phys. Chem.* **97**, 9447 (1992).
- Nakatsuji, H., Yoshimoto, M., Umemura, Y., Takagi, S., and Hada, M., *J. Phys. Chem.* **100**, 694 (1996).
- Nakatsuji, H., Yoshimoto, M., Hada, M., Domen, K., and Hirose, C., *Surf. Sci.* **336**, 232 (1995).
- Badlani, M., and Wachs, I. E., *Catal. Lett.* **75**, 137 (2001).
- Henderson, M., *J. Phys. Chem. B* **101**, 221 (1997).
- Bandara, A., Kubota, J., Wada, A., Domen, K., and Hirose, C., *J. Phys. Chem. B* **101**, 361 (1997).
- Ouyang, F., Nakayama, A., Tabada, K., and Suzuki, E., *J. Phys. Chem. B* **104**, 2012 (2000).
- Noto, Y., Fukuda, K., Onishi, T., and Tamaru, K., *Trans. Faraday Soc.* **63**, 3081 (1967).
- Cordi, E. M., O'Neill, P. J., and Falconer, J. L., *Appl. Catal. B* **14**, 23 (1997).
- Ertl, G., Knözinger, H., and Weitkamp, J., Eds., “Handbook of Heterogeneous Catalysis,” Vol. 1. VCH, Weinheim, 1997.
- Sachtler, W. M. H., and Fahrenfort, J., in “Proceedings, 2nd International Congress on Catalysis, Paris, 1960,” p. 831. Technip, Paris, 1961.
- Weast, R. C., Ed., “Handbook of Chemistry and Physics,” CRC Press, Boca Raton, FL, 1986–1987.
- Briand, L. E., Farneth, W. E., and Wachs, I. E., *Catal. Today* **62**, 2–3 (2000).
- Akhter, S., Lui, K., and Kung, H. H., *J. Phys. Chem.* **89**, 1958 (1985).
- Fukuda, K., Noto, Y., Onishi, T., and Tamaru, K., *Trans. Faraday Soc.* **63**, 3072 (1967).
- Eischens, R. P., Pliskin, W. A., in “Proceedings, 2nd International Congress on Catalysis, Paris, 1960,” p. 789. Technip, Paris, 1961.
- Boreskov, G., in “Catalysis Science and Technology” (J. R. Anderson and M. Boudart, Eds.), Vol. 3, p. 62. Springer-Verlag, New York, 1982.
- Williams, C. T., Takoudis, C. G., and Weaver, M. J., *J. Phys. Chem.* **102**, 406 (1998).
- Williams, C. T., Chan, H. Y. H., Tolia, A. A., Weaver, M. J., and Takoudis, C. G., *Ind. Eng. Chem. Res.* **37**, 2307 (1998).
- Chan, H. Y. H., Williams, C. T., Weaver, M. J., and Takoudis, C. G., *J. Catal.* **174**, 191 (1998).
- Wang, C. B., Deo, G., and Wachs, I. E., *J. Phys. Chem.* **103**, 5645 (1999).
- Knop-Gericke, A., Havecker, M., Schedel-Niedrig, T., and Schlogl, R., *Catal. Lett.* **66**, 215 (2000).
- Werner, H., Herein, D., Schulz, G., Wild, U., and Schlogl, R., *Catal. Lett.* **49**, 109 (1997).
- Deo, G., Hu, H., and Wachs, I. E., unpublished results.
- Enriquez, M. A., and Fraissard, J. P., *J. Catal.* **74**, 89 (1982).
- Poulston, S., Rowbotham, E., Stone, P., Parlett, P., and Bowker, M., *Catal. Lett.* **52**, 63 (1998).
- Burcham, L. J., and Wachs, I. E., *Catal. Today* **49**, 467 (1999).
- Hucknall, D. J., “Selective Oxidation of Hydrocarbons.” Academic Press, London, 1974.
- Turek, A. M., Wachs, I. E., and DeCanio, E., *J. Phys. Chem.* **96**, 5000 (1992).
- Perry, R. H., and Green, D. W., Eds., “Perry's Chemical Engineering Handbook,” 7th ed. McGraw-Hill, New York, 1997.
- Stubenrauch, J., Brosha, E., and Vohs, J. M., *Catal. Today* **28**, 431 (1996).
- Wachs, I. E., manuscript in preparation.
- Farneth, W. E., Staley, R. H., and Sleight, A. W., *J. Am. Chem. Soc.* **108**, 2327 (1986).